



## Evaluating the spatiotemporal dynamics of Pacific saury in the Northwestern Pacific Ocean by using a geostatistical modelling approach

Jhen Hsu <sup>a</sup>, Yi-Jay Chang <sup>a,b,\*</sup>, Toshihide Kitakado <sup>c</sup>, Mikihiko Kai <sup>d</sup>, Bai Li <sup>e</sup>, Midori Hashimoto <sup>f</sup>, Chih-hao Hsieh <sup>a,b</sup>, Vladimir Kulik <sup>g</sup>, Kyum Joon Park <sup>h</sup>

<sup>a</sup> Institute of Oceanography, National Taiwan University, No.1, Sec. 4, Roosevelt Road, Taipei 106, Taiwan

<sup>b</sup> Institute of Fisheries Science, National Taiwan University, No.1, Sec. 4, Roosevelt Road, Taipei 106, Taiwan

<sup>c</sup> Tokyo University of Marine Science and Technology, 5-7, Konan 4, Minato-ku, Tokoyo, 108-8477, Japan

<sup>d</sup> Fisheries Resources Institute, Japan Fisheries Research and Education Agency, 5-7-1 Orido, Shimizu-ku, Shizuoka-shi, 424-8633, Japan

<sup>e</sup> School of Marine Sciences, University of Maine, Orono, ME 04469, USA

<sup>f</sup> Fisheries Resources Institute, Japan Fisheries Research and Education Agency, 2-12-4 Fukuura, Kanazawa, Yokohama, Kanagawa 236-8648, Japan

<sup>g</sup> Russian Federal Research Institute of Fisheries and Oceanography, 4 Pereulok Shevchenko St., Vladivostok, 690091, Russia

<sup>h</sup> National Institute of Fisheries Science, 216,Gijanghaean-ro, Gijang-eup, Busan, 46083, Republic of Korea



### ARTICLE INFO

Handled by A.E. Punt

**Keywords:**

Pacific saury  
Spatiotemporal modelling approach  
Spatiotemporal dynamics  
Distribution shift  
Stick-held dip net fisheries

### ABSTRACT

Pacific saury (*Cololabis saira*) is an important fisheries resource and an ecologically important fish in the Northwestern Pacific Ocean. Some evidence indicates that its distribution is affected by the environmental variability, but the relative importance of environmental effects versus those of other unmodelled spatiotemporal processes has not been investigated. For this reason, fisheries data from members of the North Pacific Fisheries Commission, were analyzed using a geostatistical modelling approach to examine interannual variation in the spatiotemporal distribution of Pacific saury in the Northwestern Pacific Ocean during the fishing season (May–December) from 2001–2017. The objectives were to investigate the extent to which this can be attributed to changes in the local (e.g., sea surface temperatures), regional environmental variables (e.g., Southern Oscillation Index), and the unmodelled spatiotemporal variables (e.g., species interaction). We found that the centroid of gravity of Pacific saury had an apparent eastward shifting after 2013, and a further shift with a lower relative abundance in 2017. We also found that neither a single local or regional environmental variable nor any combination of them could explain the distributional shift of Pacific saury. Instead, the change in spatial distribution is mostly attributed to the “unmodelled” spatiotemporal variables. We emphasize that developing a quantitative understanding of the underlying mechanisms is a critical area for future work. In the future, environmental data is expected to become increasingly available. However, we caution that before projecting the Pacific saury distribution resulting from climate change or other environmental phenomena, analysts should first determine whether the hypothesized driving variables account for a meaningful proportion of variability in the historical distribution data.

### 1. Introduction

Pacific saury (*Cololabis saira*), is a small, migratory, pelagic fish, widely distributed over the extensive areas of the Northwestern Pacific Ocean (Fukushima, 1979). This species is of great commercial importance in the Northwestern Pacific Ocean, harvested mainly by stick-held dip net fisheries. Pacific saury has been internationally managed since 2015 by an inter-governmental organization, the North Pacific Fisheries Commission (NPFC), to ensure that the resource is exploited sustainably.

The offshore fishing vessels of Japan and Russia operate mainly within their domestic exclusive economic zones, whereas the distant-water vessels of China, Korea, and Taiwan operate mainly on the high seas west of 165 °E of the Northwestern Pacific Ocean.

Factors that may influence the distribution of Pacific saury have attracted considerable scientific and practical interest, as expected given its international commercial importance. The life span of Pacific saury has been estimated to be 2 years (Suyama et al., 2006). During this short life span, the population exhibits migrations between the subtropical

\* Corresponding author.

E-mail address: [yjchang@ntu.edu.tw](mailto:yjchang@ntu.edu.tw) (Y.-J. Chang).

and subarctic zones (Fukushima, 1979; Suyama et al., 2012; Miyamoto et al., 2019), and its spatial distribution appears to be affected by environmental variability in the Northwestern Pacific Ocean (Tseng et al., 2013; Chang et al., 2019; Hua et al., 2020). The specific local environmental variables previously investigated for possible effects on Pacific saury abundance and distribution have included sea surface temperature (SST; Watanabe et al., 2003; Hashimoto et al., 2020), sea surface height (SSH; Kuroda and Yokouchi, 2017), sea surface salinity (Takasuka et al., 2014), chlorophyll-a concentration (chl-a; Tseng et al., 2013) or net primary production (Chang et al., 2019), and sea surface temperature gradient (SSTG) (Hua et al., 2020). In addition, regional environmental and climatological variability (e.g., quantified by the NINO3.4 index [El Niño/Southern Oscillation indicator] and Pacific Decadal Oscillation, PDO) might also affect the distribution and density of Pacific saury (Tian et al., 2003, 2004; Chang et al., 2019). Although several previous studies have shown the possibility of forecasting potential shifts of the Pacific saury distributions using local/regional environmental variables, those studies have not shown that such variables explain a substantial portion of historical distribution shifts. For example, Tseng et al. (2011) revealed an obvious poleward shift of potential habitats of the Pacific saury under the influence of increasing SST. Chang et al. (2019) suggested that the suitable fishing grounds of Pacific saury could be predicted six months into the future by using a habitat suitability index (HSI) model including local environmental variables such as SST, SSH, SSS, and NPP. Hua et al. (2020) reported that the SSTG could explain a substantial portion of the fish density variations and provide a way to forecast Pacific saury fishing grounds based on the weight-based HSI analysis. Many studies have identified statistically significant relationships between local and/or regional environmental variables and fish density, but the relative importance of each variable in explaining the spatial distribution shifting of Pacific saury remains unclear.

The spatial distribution of Pacific saury may change due to various unmodelled spatiotemporal processes (i.e., variables that are not observed or not observable). For example, previous studies reported that the variability of Pacific saury migration might be driven by changes in prey abundance (copepods, *Neocalanus* spp.; Tadokoro et al., 2005), or complex oceanographic conditions (Saitoh et al., 1986; Tseng et al., 2014) such as eddies and fronts caused by the mixing of waters from the Kuroshio and Oyashio currents, that may trap the prey of the Pacific saury. Shifts in the distribution of Pacific saury may also be affected by interactions with other species (e.g., competition and predation) (Glaser et al., 2015; Ito et al., 2013). However, the effects of these unmodelled spatiotemporal processes that may influence the distribution shifting of Pacific saury have not yet been quantified. Recent studies suggested that the integration of simple species distribution/density models (SDMs) with the geostatistical modelling approach (i.e., Vector-Autoregressive Spatio-Temporal, VAST; Thorson, 2019) could decompose sampling variation into different biologically interpretable sources (Thorson and Barnett, 2017) and provide more precise and accurate predictions of species abundance and distribution than conventional SDMs (e.g., Shelton et al., 2014; Thorson et al., 2015). More specifically, VAST provides a more sophisticated treatment of spatiotemporal variation by accounting for both environmental and unmodelled spatiotemporal processes (i.e., species interactions, complex oceanographic condition, and fishery harvest) when estimating the species abundance and distribution.

In light of the promising features of VAST for estimating species distributions and the increasing need for understanding of the spatiotemporal dynamics of Pacific saury in the Northwestern Pacific Ocean, the objectives of this study were: (i) to evaluate the interannual spatiotemporal dynamics of Pacific saury during the fishing season (May–December) from 2001–2017 using VAST based on the data collected by the NPFC Small Scientific Committee (SSC), which comprises the most comprehensive spatiotemporal coverage currently available; (ii) to quantify the magnitude of the shift in the spatial

distribution of Pacific saury over time; (iii) to examine whether the change of spatial distribution of Pacific saury can be attributed to changes in the local and/or regional environmental variables versus the unmodelled spatiotemporal variables.

## 2. Materials and methods

### 2.1. Fishery and environmental data

The study area covered the Northwestern Pacific Ocean between 35–50 °N and 140–170 °E. Fishery data containing the catch (in metric tons) and effort (operating days) of stick-held dip net fisheries from the members of NPFC (China, Japan, Korea, Russia, Taiwan, and Vanuatu) were collected in the fishing season (May to December) during 1994–2017. The dataset was aggregated by year and month with a spatial resolution of 1° × 1° in latitude and longitude. The data were selected from 2001 to 2017 to fully cover an extensive spatial range with consistent fishing effort distribution by all members of NPFC (Supplementary Fig. S1). We assume this dataset covers the main habitat of the Pacific saury stock exploited in the Northwestern Pacific Ocean during May and December in the studied period.

We considered the local (e.g., SST) and regional environmental variables (i.e., SOI, and PDO indices) that have been most commonly used to examine possible effects on the density and distribution of Pacific saury (Tian et al., 2004; Chang et al., 2019; Hashimoto et al., 2020; Hua et al., 2020). Local environmental variables included SST (°C); SSH (m), and chl-a (mg × m<sup>-3</sup>). These local monthly environmental data were obtained from the Asia-Pacific Data Research Center (APDRC) (<http://apdrc.soest.hawaii.edu/data/data.php>) and Copernicus Marine Environment Monitoring Service (CMEMS) Global ARMOR3D L4 Reprocessed dataset (<http://marine.copernicus.eu/>). The PDO and SOI during 2001–2017 were obtained from the NOAA National Climatic Data Center (NCDC) (<https://www.ncdc.noaa.gov/>).

### 2.2. Spatiotemporal model structure

VAST (version 12.2.0) was applied to the fishery-dependent data (Xu et al., 2019; Sculley and Brodziak, 2020), expressed as catch-per-unit-effort (CPUE; measured as metric tons/operating day per square degree) to estimate the spatiotemporal dynamics of Pacific saury in the Northwestern Pacific Ocean. VAST is an R package that implements a spatiotemporal generalized linear mixed model (GLMM) framework which is publicly available online (<https://github.com/James-Thorson/VAST>). The fishing activities analyzed in this study took place in more than 250 unique 1° × 1° spatial grids. For computational efficiency, the k-means method was used to cluster all the observed data into 100 spatial knots. We then assumed that both the spatial and spatiotemporal random effects for a grid cell were established from the closest knot in space. It was confirmed that our predicted results are qualitatively similar whatever the number of spatial knots within the spatial range. The knots were allocated spatially with a density proportional to the sampling intensity according to the observation data. Ensemble knots are referred to as a mesh (Fig. 1a) and were used to approximate spatial and spatiotemporal variation, such that the spatiotemporal models predicted the density at the unsampled locations using the correlations among knots (Shelton et al., 2014). After the locations of the 100 knots were determined, they were held fixed when model parameters were estimated, and then the 0.1° × 0.1° grid cells were created as extrapolation grids to cover the whole area for the predictions in the defined spatial domain from the fitted model (Fig. 1b).

VAST implements a delta-generalized linear mixed modelling framework, where the probability distribution for catch is decomposed into two components representing the probability of encounter and the expected catch rate, given that catch occurs (Thorson, 2019). We only included the positive catch rate (i.e., observed CPUE) component because the Pacific saury schools were targeted by the stick-held dip net

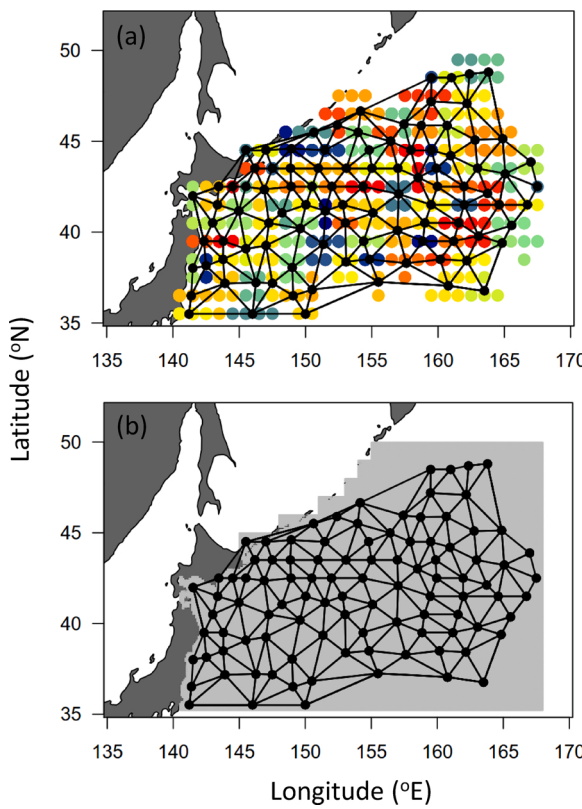


**Fig. 1.** The spatial distribution of knots and mesh used to fit the spatiotemporal model; (a) an effect is estimated for each of the 100 knots (black solid circles) in the spatiotemporal model. The colored circles grouped by knots indicate the locations of spatial observations from 2001 to 2017 within the  $1^\circ \times 1^\circ$  grid; (b) the spatial domain (grey polygon) for predicting Pacific saury density (unit: mass of fish in metric ton per day per square degree) in this study.

fisheries with 100 % encounter rate using the fish finder and satellite water temperature images. This decision is made by specifying the user-controlled vector for observation models as ObsModel = 1 (the distribution for positive catch rates is lognormal) and 3 (fixing encounter probability equals to 1 for any year) (Thorson, 2018).

The predicted Pacific saury density (i.e., mass of fish in metric ton per day per square degree) was approximated using a spatiotemporal lognormal GLMM with a log-linked linear predictor as follows:

$$p(i) = \beta(t_i) + \omega(s_i) + \varepsilon(s_i, t_i) + \sum_{j=1}^{n_j} \gamma(j) X(s_i, t_i, j) + \sum_{k=1}^{n_k} \lambda(k) Q(i, k) \quad (1)$$

where  $p(i)$  is the predictor for observation  $i$ ,  $\beta(t_i)$  is the intercept for year  $t_i$  as a fixed effect and independent among years,  $\omega(s_i)$  is time-invariant spatial variation at knot  $s_i$  (i.e., each of the 100 knots), and  $\varepsilon(s_i, t_i)$  is time-varying spatiotemporal variation for knot  $s_i$  in year  $t_i$  (i.e., the interaction of spatial variation and time). In addition,  $\gamma(j)$  is the impact of the  $j^{\text{th}}$  density covariate  $X(s_i, t_i, j)$  on knot  $s_i$  in year  $t_i$ ,  $n_j$  is the number of density covariates (in the full model,  $n_j = 8$ ),  $Q(i, k)$  is the catchability covariates that explain variation in catchability,  $\lambda(k)$  is the estimated impact of catchability covariates for this linear predictor, and  $n_k$  is the number of catchability covariates. In this study, the only catchability coefficient was a fleet dummy variable (i.e.,  $n_k = 1$ ).

The spatial and spatiotemporal variation are assumed to have correlations based on the distance from the knots; i.e., nearby densities are more similar than those that are remote. Specifically, spatial variation ( $\omega$ ) is modelled as a Gaussian random field (GRF), which reduces to a multivariate normal distribution (MVN) when evaluated at a finite set of knots (Thorson et al., 2015). The spatiotemporal random effect  $\varepsilon_t$  is fitted independently for each year and is also modelled as GRF:

$$\omega \sim MVN(0, \mathbf{R}_\omega) \quad (2a)$$

$$\varepsilon_t \sim MVN(0, \mathbf{R}_\varepsilon) \quad (2b)$$

where MVN is the multivariate normal distribution with expected value 0 for each knot;  $\mathbf{R}$  is a covariance matrix for the random field. We assumed the covariance between two knots  $s$  and  $s'$  follow the Matérn correlation function:

$$\mathbf{R}_\omega(s, s') = \text{Matern}(\kappa |H(s - s')|) \quad (3a)$$

$$\mathbf{R}_\varepsilon(s, s') = \text{Matern}(\kappa |H(s - s')|) \quad (3b)$$

where  $\kappa$  determines the rate at which decorrelation drops with increasing distance, and  $H$  is a  $2 \times 2$  linear transformation matrix representing geometric anisotropy (a condition where spatial correlation varies with both and distance and direction; see Thorson et al., 2015). The marginal likelihood of fixed effect parameters is calculated with Template Model Builder using the Laplace approximation to integrate across random effect parameters (Kristensen et al., 2016), and fixed effect parameters are then estimated by maximizing the marginal likelihood within the R computing environment (R Core Team, 2018). The standard errors of estimated parameters and model outputs were calculated using the generalization of the delta method (Kass and Stefey, 1989). Convergence was checked by ensuring that the absolute value of the final gradient of the log-likelihood function at the maximum likelihood estimate was less than 0.0001 for all parameters and that the Hessian matrix of the likelihood function was positive definite.

### 2.3. Density covariates

Five density covariates were retained in the best (i.e., most parsimonious) model based on backward model selection using the Akaike Information Criterion (AIC) (Akaike, 1974) in the preliminary analyses, where a variable was excluded from the model if the AIC was lower after removing the variable from the full model of each batch (Supplementary Table S1):

$$X(s, t) = (\text{SST}(s, t), \text{SST}^2(s, t), \text{chl-a}(s, t), \text{SOI}(s(N), t), \text{SOI}(s(E), t)) \quad (4)$$

where  $\text{SST}(s, t)$  is the linear effect of sea surface temperature associated with knot  $s$  and year  $t$ ,  $\text{SST}^2(s, t)$  is temperature-squared (i.e., a quadratic effect of temperature),  $\text{chl-a}(s, t)$  is the concentration of chlorophyll-a.  $\text{SOI}(s(N), t)$ , and  $\text{SOI}(s(E), t)$  are the interaction of northward (latitudinal) or eastward (longitudinal) direction with the annual trend of SOI index (Thorson et al., 2017a). The low correlations among the density covariates (Pearson's correlation coefficients ranging from -0.03–0.13), and the nonlinear relationship between SST and  $\text{SST}^2$  indicated that the multicollinearity is not an issue for the best model.

### 2.4. Derived index of relative abundance

The index of relative abundance in year  $t$ , computed using an area-weighted approach,  $B(t)$ , was obtained by scaling the predicted density by the total area associated with the knots (Thorson et al., 2015):

$$B(t) = \sum_{s=1}^{n_s} a(s) \times \exp \left( \beta(t) + \omega(s) + \varepsilon(s, t) + \sum_{j=1}^{n_j} \gamma(j) X(s, t, j) \right) \quad (5)$$

where  $n_s$  denotes the number of knot  $s$  (i.e.,  $n_s = 100$ ), and  $a(s)$  is the area associated with modelled knot  $s$ .

### 2.5. Calculating the centroid of gravity

To summarize the distribution shift for Pacific saury during the

studied period, we calculated a model-based estimate of the yearly ( $t$ ) centroid of gravities (COG $_t$ ) from the predicted relative abundance throughout the whole spatial domain (Thorson et al., 2017a):

$$COG_t = \sum_{s=1}^{n_s} \frac{\hat{B}_t \times Z_s}{\hat{B}_t} \quad (6)$$

where  $Z_s$  is the northing or easting value for knot  $s$  in the Universal Transverse Mercator (UTM) coordinate in kilometers (km), and  $\hat{B}_t$  is the predicted relative abundance in the year  $t$ .

## 2.6. Counterfactual model exploration

The spatiotemporal random fields,  $\varepsilon(s, t)$ , and the covariates,  $X(s, t, j)$ , in VAST can account for changes in spatial distribution over time. The spatiotemporal random fields representing the unmodelled spatiotemporal processes could capture residual patterns that cannot be attributed to the fixed effects (i.e., the covariates). Therefore, to examine the relative importance of the local and/or regional environmental variables versus the unmodelled spatiotemporal variables for explaining the spatial distribution shift of Pacific saury, a counterfactual analysis (Thorson et al., 2017a; Perretti and Thorson, 2019) was conducted. We evaluated the following three hypotheses for changes in the distribution of Pacific saury over time: (i) single local or regional environmental variable; (ii) multiple local and regional environmental variables; and (iii) unmodelled spatiotemporal variables. These hypotheses are not mutually independent; thus we seek to estimate what proportion of variance in COG is explained by each of these variables. More specifically, the estimates of fixed and random effects were extracted from the best model, and some were fixed to zero to exclude individual processes from the model. For each counterfactual model, the time series of northward and eastward COG from the estimation without the subset of the parameters were then compared to the COG derived from the best model. In an exploratory run, we confirm that fixing both environmental variables and unexplained variation at zero results in no variance in COG. This confirms that all estimated variation in COG is attributable to one of these two processes. The details about quantitative descriptions for the counterfactual models are described as below:

### 2.6.1. Single local or regional environmental variable

To examine the relative effect of a single local (i.e., SST, SST<sup>2</sup>, chl-a) or regional (i.e., SOI index with northing and easting) environmental variables, the intercept was fixed at the average level across time, and any variation of the spatiotemporal random effect was removed. Only one of the estimated single local variables or a regional environmental variable was retained at a time to predict relative abundance and recalculate the COG. Descriptions of the mechanism and the quantitative test for the hypothesis of the distribution shift are provided in Table 1.

### 2.6.2. Multiple local and regional environmental variables

The intercept was fixed at the average level over time, and the variation from the spatiotemporal random effect (i.e., set at zero) was removed to examine the relative effect of multiple local and regional environmental variables. Combinations of local and regional environmental variables were then set to their estimated values, which were used to predict the relative abundance for all knots, and recalculate the COG.

### 2.6.3. Unmodelled spatiotemporal variables

To examine the relative effect of the unmodelled spatiotemporal processes (which was not explained by any local/regional environmental variables), any effects from the local/regional environmental variables were eliminated, and the steps above were followed to recalculate relative abundance and COG.

**Table 1**

Mechanisms and quantitative tests of each hypothesized driver that may affect the distribution of Pacific saury in the Northwestern Pacific Ocean.

Hypothesized drivers	Description of mechanism	Quantitative test for the hypothesis
Single local or regional environmental variable	Variation in a single regional (e.g., SST) or regional environmental variable drives interannual changes in distribution	<ol style="list-style-type: none"> <li>Fixing the intercepts at their average values across years: <math>\bar{\beta} = n_t^{-1} \sum_{t=1}^{n_t} \beta(t)</math>;</li> <li>Retaining the residual spatial variation: <math>\omega(s)</math>;</li> <li>Fixing the residual spatiotemporal variation at zero: <math>\varepsilon(s, t) = 0</math>;</li> <li>Retaining the coefficient of a single local (e.g., SST) or regional environmental variable and fixing the impact of subset local/regional environmental variable at zero.</li> </ol>
Multiple local and regional environmental variables	Variation in all local and regional environmental variables drives interannual changes in distribution	<ol style="list-style-type: none"> <li>Fixing the intercepts at their average values across years: <math>\bar{\beta} = n_t^{-1} \sum_{t=1}^{n_t} \beta(t)</math>;</li> <li>Retaining the residual spatial variation: <math>\omega(s)</math>;</li> <li>Fixing the residual spatiotemporal variation at zero: <math>\varepsilon(s, t) = 0</math>;</li> <li>Retaining the coefficients of all local and regional environmental variables.</li> </ol>
Unmodelled variable	Otherwise unmodelled processes (e.g., the shift in the spatial distribution of predators or food availability) drive interannual changes in distribution	<ol style="list-style-type: none"> <li>Fixing the intercepts at their average values across years: <math>\bar{\beta} = n_t^{-1} \sum_{t=1}^{n_t} \beta(t)</math>;</li> <li>Retaining the residual spatial variation: <math>\omega(s)</math>;</li> <li>Retaining the residual spatiotemporal variation;</li> <li>Fixing the coefficients of all local and regional environmental variables at zero: <math>\sum_{j=1}^{n_j=5} \gamma_j = 0</math>.</li> </ol>

## 3. Results

### 3.1. Spatiotemporal dynamics of Pacific saury

VAST fit the data robustly, as indicated by the goodness of fit of the best model (deviance explained = 69%). The time series of residuals across knots are around zero (Supplementary Fig. S2), and the spatial distribution of residuals showed no substantial spatial pattern, except during 2005 and 2006 (Supplementary Fig. S3). All environmental variables included in the best model were statistically significant (likelihood ratio test,  $P < 0.001$ ). The estimate of the standard deviation for the spatiotemporal random effect had a significantly greater magnitude (0.543) than that of the spatial random effect (0.283), which reflected heterogeneity in the spatial distribution of density in the Pacific saury over time. Geometric anisotropy spatial correlation of the Pacific saury density is summarized in Fig. 2. The correlation ellipse (i.e., 10% correlation distance) is oriented from east to west or vice versa, signifying that the related spatial and spatiotemporal correlations of the Pacific saury density decreased faster latitudinally than longitudinally.

The predicted density maps from the best model showed that Pacific saury exhibited substantial interannual variation in density distribution during 2001–2017 (Fig. 3). In the early years (2001–2007), the high densities mostly occurred near the coastal waters of Japan (140–150°E and 38–45°N), except for 2005. However, the area of high density has

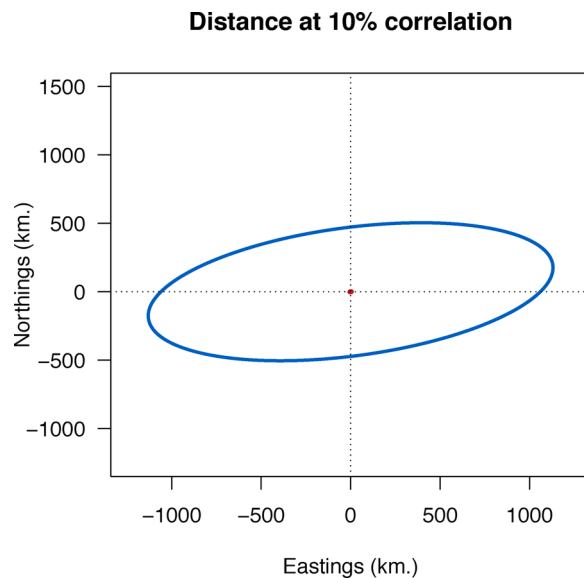


**Fig. 2.** The magnitude of 2-dimensional spatial autocorrelation for Pacific saury distribution. The ellipse signifies the distance (from a point located at position (0,0)), where the correlation drops to 10 %. For instance, an ellipse that is stretched East-West signifies that the predicted density is correlated over a longer distance moving East-West than North-South.

generally shifted and expanded eastward since the start of 2010, and an apparent eastward shift was observed after 2013. The high densities during 2015–2017, occurred in the high seas ( $150\text{--}160^{\circ}\text{E}$  and  $40\text{--}45^{\circ}\text{N}$ ). We noted that the predicted density distribution in 2017 was substantially different from those in the previous years; that is, high density appears in the area of  $150\text{--}170^{\circ}\text{E}$  and  $36\text{--}42^{\circ}\text{N}$  in 2017. Furthermore, the predicted time series of annual density from the best model showed a fluctuating pattern, and similar trends were observed for the nominal CPUE and the predicted relative abundance (Fig. 4).

### 3.2. Time series of COGs of Pacific saury

The trajectories of the northward and eastward COG from the best model (Fig. 5a, b) also indicated an apparent eastward shift in distribution (the maximum difference is 585 km) compared to the north-south direction (146 km) over the years. The eastward COG in 2006 and 2017 reached the historical minimum and maximum easting of 175 km and 760 km, respectively (Fig. 5a). COG has gradually shifted eastward since 2010 and further shifted after 2013. For the north-south direction, the time series of COG indicated relatively persistent regimes in the distribution (Fig. 5b). The 95 % confidence intervals of the eastward COGs were wider (CV range = 6.4 %–27.8 %) than those of the northward direction (CV range = 0.4 %–1.1 %) throughout the study period, reflecting greater spatial variability of density longitudinally than latitudinally.

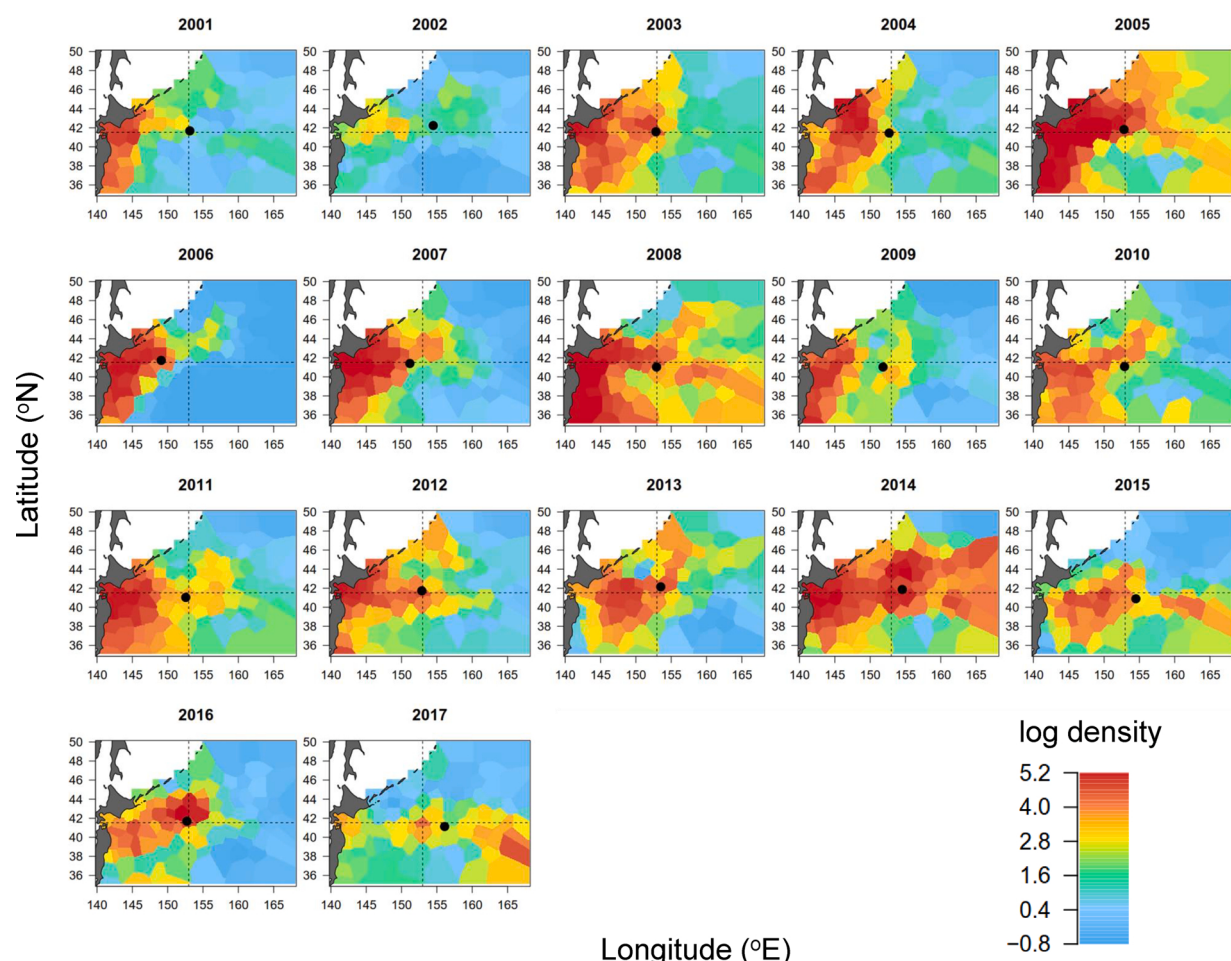


**Fig. 3.** Spatiotemporal distributions of the log-transformed density of Pacific saury (unit: mass of fish in metric ton per day per square degree) from 2001 to 2017. The black circle is the location of the estimated centroid of gravity (COG). The dashed line represents the average location of the estimated centroid of gravity (COG).

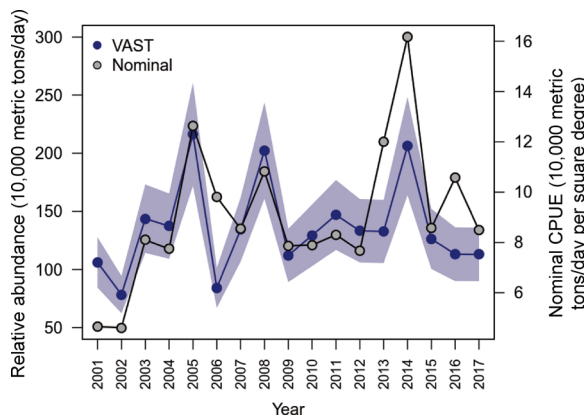


**Fig. 4.** The time-series of the index of relative abundance (metric ton/day) from VAST for Pacific saury in the Northwestern Pacific Ocean during 2001–2017. The blue polygon represents the 95 % confidence interval. The grey circle represents the nominal catch-per-unit-effort, CPUE (metric ton/day per square degree).

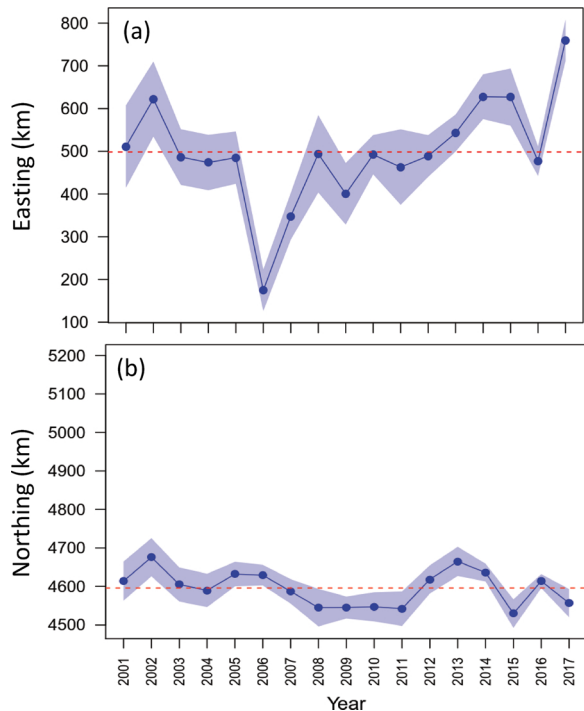


**Fig. 5.** The time-series of the estimated centroids of gravities (COGs) in the (a) easting and (b) northing directions from the spatiotemporal model during 2001–2017. The red dashed line represents the average COG over the year; the blue polygon represents the 95 % confidence interval.

### 3.3. Relative importance of local/regional environmental vs. unmodelled variables

The predicted density maps for 2001, 2006, 2010, and 2017, which represent the most substantial inconsistencies among the counterfactual models were selected to illustrate the relative importance of local/regional environmental and unmodelled spatiotemporal variables (Fig. 6). Decomposing the relative influence(s) of a single local or regional environmental variable, the results indicated that SST in isolation (i.e., linear and quadratic SST) could not explain the interannual variation of the density distribution (i.e., neither high-density areas nor yearly variation) derived from the best model (Fig. 6a, b). Similar results were found for the other covariates except for the SOI

index with northings (Supplementary Fig. S4). Multiple environmental variables and climatic indices in isolation led to a similar pattern of the density distribution compared to that by the SOI index with northings (Fig. 6c; Supplementary Fig. S4e). The general patterns in the spatio-temporal variation of density are mainly attributed to the unmodelled spatiotemporal variable (Fig. 6d), although unmodelled spatiotemporal variable in isolation could overestimate density in 2010 and 2017 compared to other covariates.

Investigation of the estimated COG trends under each hypothesized driver clearly confirms that the observed interannual variation in COG was mainly due to unmodelled variation. The COG trends (both easting and northing directions) derived from the unmodelled spatiotemporal variable in isolation were similar to those from the best model in both directions (Fig. 7). SST generated flat COG trends (Fig. 7c, d), which indicated that SST has very limited prediction power for the Pacific saury density. The SOI index with northings contributed to relatively larger fluctuations in COGs than the other local/regional environmental variables (Supplementary Figs. S5, S6). This result suggests that the SOI index is the most important factor among the local/regional variables in explaining the interannual spatial distribution patterns (Supplementary Figs. S5f, S6f). The COG trends derived from the multiple environmental variables and climatic indices were similar to that by the SOI index with northings (Supplementary Figs. S5b, f and S6b, f). It should be noted that the COG trends could be balanced out by the offset effects among the local and regional environmental variables, which led to a less varied COG trend along the north-south axis over time (Fig. 7e, f).

### 4. Discussion

We analyzed spatiotemporal dynamics of Pacific saury density in the Northwest Pacific Ocean between 35–50 °N and 140–170 °E during 2001–2017 by using the VAST R package and the extensive fishery dataset collected by the NPFC SSC. We note that use of fishery-dependent data collected without a scientific sampling design may lead to the CPUE data from preferred fishing grounds having a disproportionate influence on the predicted density distribution, which is often referred to as preferential sampling (Conn et al., 2017; Diggle et al., 2007; Gao et al., 2020). For the Pacific saury, this may not be a serious problem because the data used in this study were collected with a consistent fishing effort distribution for each member of the NPFC. Also, this joint fishery data from all members covers an extensive spatial range for the studied period. In addition, VAST is a better way to reduce the bias and variance than a nonspatial modelling approach because of its ability to account for correlated spatial processes, predict densities in unfished areas via imputation, and implement an appropriate area-weighting scheme (Thorson et al., 2015). We also recommend ongoing work to develop an approach to estimate fisher locational decisions and fish densities simultaneously (Thorson et al., 2017b).

The area of high density and COG has gradually shifted eastward since 2010 and further shifted after 2013. The eastward distribution shift was additionally accompanied by a relatively low density in 2017. The eastward shift in Pacific saury distribution after 2010 was also identified based on fishery-independent biomass surveys (Hashimoto et al., 2020). We found that neither a single local or regional environmental variable nor any linear combination could explain the Pacific saury distribution shifts. Instead, most of the distribution shift was attributed to the unmodelled spatiotemporal variation. This result is consistent with the findings from previous studies using conventional SDMs (e.g., regression-based models) that have attributed a small portion of the data variability in distribution variation for Pacific saury to the investigated environmental effects (e.g., deviance explained <36 % in Tseng et al., 2013; <12 % in Chang et al., 2019). Instead, VAST, conditioning on unmodelled spatiotemporal variables that are informed as the random effects (Thorson and Ward, 2013; Shelton et al., 2014) is able to capture residual spatiotemporal patterns that cannot be attributed to the fixed effects (e.g., the environmental variables). In the

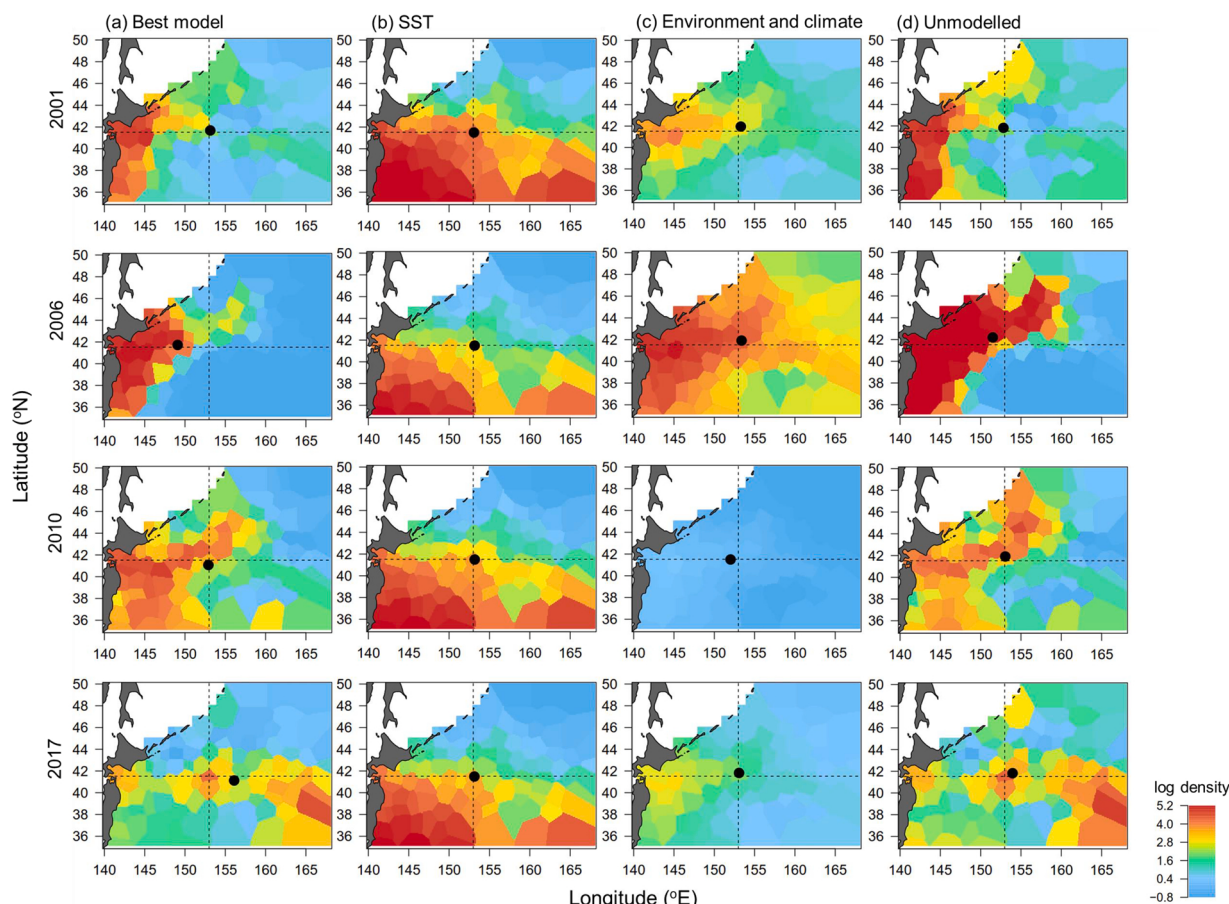


**Fig. 6.** Estimated log-density (unit: mass of fish in metric ton per day per square degree) in 2001, 2006, 2010, and 2017 for the Pacific saury from the best model (a). Each hypothesized driver that eliminates all causes for variation in distribution except the SST (b), the multiple local and regional environmental variables (c), and the unmodelled variable (d). The black circle represents the location of the estimated centroid of gravity (COG) for each model. The dashed line represents the average location of the estimated centroid of gravity (COG) from the best model.

future, environmental data should become increasingly available. However, we caution that before projecting the Pacific saury distribution resulting from climate change or other environmental phenomena, the first step should be to verify whether the hypothesized driving variables lead to a meaningful proportion of variability in the historical distribution data.

There are several possible mechanisms to explain why the shifts in Pacific saury distribution are attributed to the “unmodelled” spatiotemporal variation. For example, *Neocalanus* copepods are the common zooplankton prey for the Japanese sardine (*Sardinops melanostictus*) and Pacific saury (Tadokoro et al., 2005). Ito et al. (2013) indicated that the increase in the abundance of Japanese sardine could lead to a decrease in the prey plankton density and hence the growth of Pacific saury. It is worth noting that the stock of Japanese sardines increased steadily after 2013 (Furuichi et al., 2019). We hypothesize that the spatiotemporal variation in the density of Pacific saury may be strongly correlated (negative) with the effect of the competitive fish species (i.e., Japanese sardine) on the zooplankton prey of Pacific saury (Matsuda et al., 1992). Although only a single species distribution model was constructed in this study, VAST can analyze data for multiple species simultaneously to infer the spatiotemporal variation in the density of species with similar habitat requirements. Thorson and Barnett (2017) reported that there was a strong covariation in population density among US Pacific Coast rockfishes and thornyheads (*Sebastodes* and *Sebastolobus* spp.) using joint species distribution prediction. We suggest that using this modelling technique may improve estimation of the population density distribution of Pacific saury while considering other correlated fish species when multiple species data are available.

Previous studies suggested that complicated hydrographical dynamics (e.g., fronts and eddies) may result in spatial distribution shifts of Pacific saury over time. Yasuda and Watanabe (1994) showed that the interannual north-south shift of the Oyashio front is relevant to the interannual fluctuation of the fishing grounds of Pacific saury. Kuroda et al. (2017) revealed that the peculiarities of the interactions between the Oyashio current and mesoscale eddies after 2010 led a shift in the large areas of favorable potential fishing ground from the Hokkaido coast to offshore in recent years. Although the spatial distribution of Pacific saury is difficult to explain using local/regional environmental variables, we consider that the possible effect of the hydrographical dynamics on the distribution shifts of Pacific saury could be captured by the unmodelled spatiotemporal variable in the model.

The catches of the Pacific saury were limited to the Japanese EEZ in the early period (2001–2007). However, there is an increasing trend of fishing mortality after 2007 attributed to the increase of catches in high-seas areas (NPFC, 2019). We recommend future research to integrate the spatial information regarding the fishing mortality as a density covariate into the current spatiotemporal model to explore whether the eastward shift of density distribution primarily attributed to the unmodelled variation can be related to the heterogeneity in fishing intensity.

There are several possible explanations for the inability of the effects of local/regional environmental variables to explain Pacific saury distribution shifts. One is that the model could not capture the effect of the local/regional environmental variables due to the insufficient model flexibility. Nevertheless, we included a quadratic effect of the local environmental variable (SST) and a linear effect of the regional environmental variable (SOI). It is possible that a highly nonlinear model (e.

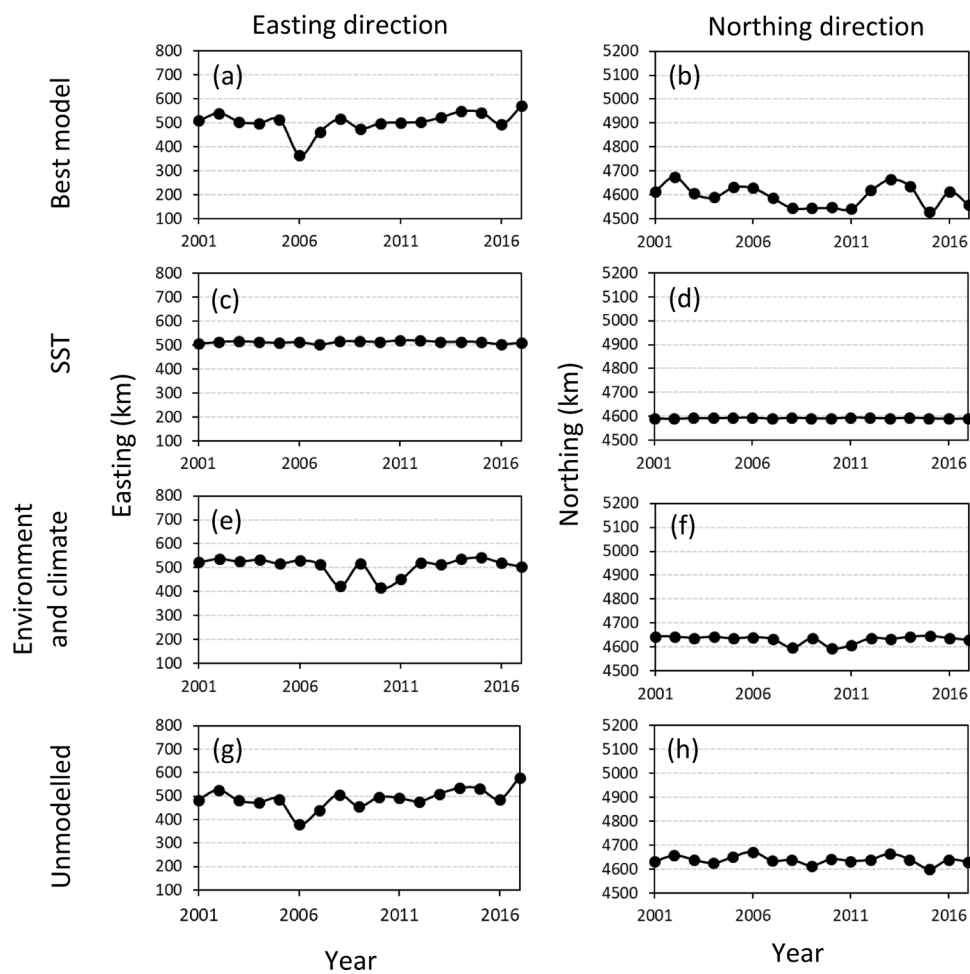


**Fig. 7.** The estimated centroids-of-gravity (COGs) during 2001–2017 for the Pacific saury from the best model (a, b) in easting and northing directions, compared to those from each hypothesized driver that eliminates all causes for variation in distribution except SST (c, d), the multiple local and regional environmental variables (e, f), and the unmodelled variable (g, h).

., spline) may improve the model performance. However, we caution that adding more flexible model structures may lead to spurious relationships, which could be mistaken as meaningful (Fourcade et al., 2018). Furthermore, previous studies indicated that the abundance and the suitable spawning ground of the Pacific saury exhibited interannual-decadal variation due to regime shifts (Ichihi et al., 2017; Liu et al., 2019). Including the interactions of environmental variables and an additional dummy variable or spatially-varying coefficient models (Li et al., 2018; Thorson, 2019) may increase the estimated importance of some environmental variables, although this was outside the scope of this study. Chang et al. (2019) indicated that habitat preferences and suitable habitat areas of Pacific saury differed between size classes (e.g., medium- and large-sized). The age/size aggregated model with the spatiotemporal random effects used in this study may balance out the estimated importance of local or regional environmental variables. We recommend that adding (currently unavailable) age/size data may provide additional information to better understand the ontogenetic habitat preferences combined with changes in age/size structure of Pacific saury and improve the estimated importance of the environmental variables (Kristensen et al., 2014; Kai et al., 2017; Barbeaux and Hollowed, 2018).

Knowledge of the spatiotemporal dynamics of Pacific saury may allow for the use of spatially explicit stock assessment models for future work. This is important because the current Bayesian surplus production model used for assessment of the Pacific saury by NPFC does not take the spatial structure in population dynamics into account. Punt (2019)

indicated that including the pre-processing data with the spatial modelling approach (Cao et al., 2017; Kai et al., 2017) is one of the approaches to incorporate the spatial structure in assessment models. Although this study has produced a time series of density index using VAST, we did not focus on the use of the standardized index of relative abundance for stock assessment purposes. Calculating the annual standardized index requires considering the confounding factors, such as seasonal effects, vessel-specific effects, and change in target species that may (Li et al., 2018) influence catchability. We recommend that future research should focus on simulations that investigate the merits of using spatiotemporal model under varying scenarios about fish abundance trends and the distribution of fish and fishing effort across time and space, as well as the performance of the standardized index for improving confidence in stock assessment outcomes. Finally, it is important to monitor the eastward shift of the “hotspot” in Pacific saury density (i.e., COG) over time. Hotspots are frequently used in conservation efforts when planning spatial protection (e.g., time-area closure) of harvested species, and changes over time in the location of hotspots have profound implications for the usefulness of these spatial protections.

#### CRediT authorship contribution statement

**Jhen Hsu:** Conceptualization, Methodology, Software, Writing - original draft. **Yi-Jay Chang:** Conceptualization, Methodology, Software, Writing - review & editing. **Toshihide Kitakado:** Methodology,

Writing - review & editing. **Mikihiko Kai:** Methodology, Software, Writing - review & editing. **Bai Li:** Writing - review & editing. **Midori Hashimoto:** . **Chih-hao Hsieh:** Methodology, Writing - review & editing. **Vladimir Kulik:** Writing - review & editing. **Kyum Joon Park:** Writing - review & editing.

## Declaration of Competing Interest

We have no conflict of interest to declare.

## Acknowledgements

The authors thank the members of the Small Scientific Committee on Pacific Saury of the North Pacific Fisheries Commission for the use of their data. We thank Chris Rooper and Jie Cao who have both contributed to discussions regarding the spatial modelling approach, Kazuhiro Oshima, Satoshi Suyama, Shin-Ichiro Nakayama, Taiki Fuji, Wen-Bin Huang, Yong Chen, Siquan Tian, and Chuanxiang Hua for their comments on this study, Aleksandr Zavolokin and Mervin Ogawa for ongoing help and maintenance for the joint Pacific saury fisheries and oceanography database. We also thank William Walsh for the manuscript editing. We are grateful to two anonymous reviewers and editor, André Punt, who provided helpful comments and edits that improved this manuscript. This study was partially financially supported by the Ministry of Science and Technology and the Fishery Agency of Council of Agriculture of Taiwan through the research grants 109–2611–M–002–013– and 109AS–9.1.4–FA–F1 to Yi-Jay Chang.

## Appendix A. Supplementary data

Supplementary material related to this article can be found, in the online version, at doi:<https://doi.org/10.1016/j.fishres.2020.105821>.

## References

- Akaike, H., 1974. New look at statistical-model identification. *IEEE Trans. Autom. Control* AC19, 716–723.
- Barbeaux, S.J., Hollowed, A.B., 2018. Ontogeny matters: climate variability and effects on fish distribution in the eastern Bering Sea. *Fish. Oceanogr.* 27, 1–15.
- Cao, J., Thorson, J.T., Richards, R.A., Chen, Y., 2017. Spatiotemporal index standardization improves the stock assessment of northern shrimp in the Gulf of Maine. *Can. J. Fish. Aquat. Sci.* 74, 1781–1793.
- Chang, Y.J., Lan, K.W., Walsh, W.A., Hsu, J., Hsieh, C.H., 2019. Modelling the impacts of environmental variation on habitat suitability for Pacific saury in the Northwestern Pacific Ocean. *Fish. Oceanogr.* 28, 291–304.
- Conn, P.B., Thorson, J.T., Johnson, D.S., 2017. Confronting preferential sampling when analysing population distributions: diagnosis and model-based triage. *Methods Ecol. Evol.* 8 (11), 1535–1546.
- Diggle, P., Ribeiro, P., Geostatistics, M.–b., 2007. Springer Series in Statistics. Springer.
- Fournade, Y., Besnard, A.G., Secondi, J., 2018. Paintings predict the distribution of species, or the challenge of selecting environmental predictors and evaluation statistics. *Glob. Ecol. Biogeogr.* 27, 245–256.
- Fukushima, S., 1979. Synoptic analysis of migration and fishing conditions of saury in the northwest Pacific Ocean. *Bull. Tohoku Reg. Fish. Res. Lab.* 41, 1–70.
- Furuichi, S., Watanabe, C., Yukami, R., Kamimura, Y., Isu, S., 2019. Stock assessment and evaluation for Japanese sardine (Pacific stock) (fiscal year 2018). Marine Fisheries Stock Assessment and Evaluation for Japanese Waters (fiscal Year 2018/2019). Fisheries Agency and Fisheries Research and Education Agency of Japan, pp. 14–56. <http://abchan.fra.go.jp/>.
- Gao, J., Thorson, J.T., Szuwalski, C., Wang, H.Y., 2020. Historical dynamics of the demersal fish community in the East and South China Seas. *Mar. Freshwater Res.* 71 (9), 1073–1085.
- Glaser, S.M., Waechter, K.E., Bransome, N.C., 2015. Through the stomach of a predator: regional patterns of forage in the diet of albacore tuna in the California current System and metrics needed for ecosystem–based management. *J. Mar. Syst.* 146, 38–49.
- Hashimoto, M., Kidokoro, H., Suyama, S., Fuji, T., Miyamoto, H., Naya, M., Kitakado, T., 2020. Comparison of biomass estimates from multiple stratification approaches in a swept area method for Pacific saury *Cololabis saira* in the western North Pacific. *Fish. Res.* 1–12.
- Hua, C., Li, F., Zhu, Q., Zhu, G., Meng, L., 2020. Habitat suitability of Pacific saury (*Cololabis saira*) based on a yield–density model and weighted analysis. *Fish. Res.* 221, 105408.
- Ichii, T., Nishikawa, H., Igarashi, H., Okamura, H., Mahapatra, K., Sakai, M., Okada, Y., 2017. Impacts of extensive driftnet fishery and late 1990s climate regime shift on dominant epipelagic nekton in the Transition Region and Subtropical Frontal Zone: implications for fishery management. *Prog. Oceanogr.* 150, 35–47.
- Ito, S.I., Okunishi, T., Kishi, M.J., Wang, M., 2013. Modelling ecological responses of Pacific saury (*Cololabis saira*) to future climate change and its uncertainty. *ICES J. Mar. Sci.* 70, 980–990.
- Kai, M., Thorson, J.T., Piner, K.R., Maunder, M.N., 2017. Predicting the spatio-temporal distributions of pelagic sharks in the western and central North Pacific. *Fish. Oceanogr.* 26, 569–582.
- Kass, R.E., Steffey, D., 1989. Approximate Bayesian inference in conditionally independent hierarchical models (parametric empirical Bayes models). *J. Am. Stat. Assoc.* 84, 717–726.
- Kristensen, K., Thygesen, U.H., Andersen, K.H., Beyer, J.E., 2014. Estimating spatiotemporal dynamics of size–structured populations. *Can. J. Fish. Aquat. Sci.* 71, 326–336.
- Kristensen, K., Nielsen, A., Berg, C.W., Skaug, H., Bell, B.M., 2016. TMB: automatic differentiation and laplace approximation. *J. Stat. Softw.* 70, 1–21.
- Kuroda, H., Yokouchi, K., 2017. Interdecadal decrease in potential fishing areas for Pacific saury off the southeastern coast of Hokkaido, Japan. *Fish. Oceanogr.* 26, 439–454.
- Li, B., Cao, J., Guan, L., Mazur, M., Chen, Y., Wahle, R.A., 2018. Estimating spatial non-stationary environmental effects on the distribution of species: a case study from American lobster in the Gulf of Maine. *ICES J. Mar. Sci.* 75 (4), 1473–1482.
- Liu, S., Liu, Y., Fu, C., Yan, L., Xu, Y., Wan, R., Tian, Y., 2019. Using novel spawning ground indices to analyze the effects of climate change on Pacific saury abundance. *J. Mar. Syst.* 191, 13–23.
- Matsuda, H., Wada, T., Takeuchi, Y., Matsumiya, Y., 1992. Model analysis of the effect of environmental fluctuation on the species replacement pattern of pelagic fishes under interspecific competition. *Res. Popul. Ecol.* 34, 309–319.
- Miyamoto, H., Suyama, S., Vijai, D., Kidokoro, H., Naya, M., Fuji, T., Sakai, M., 2019. Predicting the timing of Pacific saury (*Cololabis saira*) immigration to Japanese fishing grounds: a new approach based on natural tags in otolith annual rings. *Fish. Res.* 209, 167–177.
- Perretti, C.T., Thorson, J.T., 2019. Spatiotemporal dynamics of summer flounder (*Paralichthys dentatus*) on the Northeast US shelf. *Fish. Res.* 215, 62–68.
- Punt, A.E., 2019. Spatial stock assessment methods: a viewpoint on current issues and assumptions. *Fish. Res.* 213, 132–143.
- R Core Team, 2018. R: A Language and Environment for Statistical Computing [online]. R Foundation For Statistical Computing, Vienna, Austria. Available from <http://www.R-project.org/>.
- Saitoh, S.I., Kosaka, S., Isaka, J., 1986. Satellite infrared observations of Kuroshio warm–core rings and their application to study of Pacific saury migration. *DEEP–SEA Res. PT. I.* 33, 1601–1615.
- Sculley, M.L., Brodziak, J., 2020. Quantifying the distribution of swordfish (*Xiphias gladius*) density in the Hawaii–based longline fishery. *Fish. Res.* 230, 105638.
- Shelton, A.O., Thorson, J.T., Ward, E.J., Feist, B.E., 2014. Spatial semiparametric models improve estimates of species abundance and distribution. *Can. J. Fish. Aquat. Sci.* 71, 1655–1666.
- Suyama, S., Morioka, T., Nakaya, M., Nakagami, M., Ueno, Y., 2006. The study of the maturation process of the Pacific saury, *Cololabis saira*: the role of the rearing experiments. *Bull. Fish. Res. Agency (Japan)*.
- Suyama, S., Nakagami, M., Naya, M., Ueno, Y., 2012. Migration route of Pacific saury *Cololabis saira* inferred from the otolith hyaline zone. *Fish. Sci.* 78, 1179–1186.
- Tadokoro, K., Chiba, S., Ono, T., Midorikawa, T., Saino, T., 2005. Interannual variation in *Neocalanus* biomass in the Oyashio waters of the western North Pacific. *Fish. Oceanogr.* 14, 210–222.
- Takasuka, A., Kuroda, H., Okunishi, T., Shimizu, Y., Hirota, Y., Kubota, H., Sakaji, R., Kimura, R., Ito, S.I., Oozeki, Y., 2014. Occurrence and density of Pacific saury *Cololabis saira* larvae and juveniles in relation to environmental factors during the winter spawning season in the Kuroshio Current system. *Fish. Oceanogr.* 23 (4), 304–321.
- Technical Working Group on Pacific Saury Stock Assessment, 2019. 4<sup>th</sup> Meeting Report. NPFC–2019–TWG PSSA04–Final Report, p. 50 pp. [www.npfc.int](http://www.npfc.int).
- Thorson, J.T., 2018. VAST User Manual. <https://github.com/James-Thorson-NOAA/VAST/tree/master/manual>.
- Thorson, J.T., 2019. Guidance for decisions using the Vector Autoregressive Spatiotemporal (VAST) package in stock, ecosystem, habitat and climate assessments. *Fish. Res.* 210, 143–161.
- Thorson, J.T., Barnett, L.A., 2017. Comparing estimates of abundance trends and distribution shifts using single– and multispecies models of fishes and biogenic habitat. *ICES J. Mar. Sci.* 74, 1311–1321.
- Thorson, J.T., Ward, E.J., 2013. Accounting for space–time interactions in index standardization models. *Fish. Res.* 147, 426–433.
- Thorson, J.T., Shelton, A.O., Ward, E.J., Skaug, H.J., 2015. Geostatistical delta–generalized linear mixed models improve precision for estimated abundance indices for West Coast groundfishes. *ICES J. Mar. Sci.* 72, 1297–1310.
- Thorson, J.T., Ianelli, J.N., Kotwicki, S., 2017a. The relative influence of temperature and size-structure on fish distribution shifts: a case-study on Walleye pollock in the Bering Sea. *Fish. Fish. (Oxf.)* 18, 1073–1084.
- Thorson, J.T., Fonner, R., Haltuch, M.A., Ono, K., Winker, H., 2017b. Accounting for spatiotemporal variation and fisher targeting when estimating abundance from multispecies fishery data. *Can. J. Fish. Aquat. Sci.* 74 (11), 1794–1807.
- Tian, Y., Akamine, T., Suda, M., 2003. Variations in the abundance of Pacific saury (*Cololabis saira*) from the northwestern Pacific in relation to oceanic–climate changes. *Fish. Res.* 60, 439–454.

- Tian, Y., Ueno, Y., Suda, M., Akamine, T., 2004. Decadal variability in the abundance of Pacific saury and its response to climatic/oceanic regime shifts in the northwestern subtropical Pacific during the last half century. *J. Mar. Syst.* 52, 235–257.
- Tseng, C.T., Sun, C.L., Yeh, S.Z., Chen, S.C., Su, W.C., Liu, D.C., 2011. Influence of climate-driven sea surface temperature increase on potential habitats of the Pacific saury (*Cololabis saira*). *ICES J. Mar. Sci.* 68, 1105–1113.
- Tseng, C.T., Su, N.J., Sun, C.L., Punt, A.E., Yeh, S.Z., Liu, D.C., Su, W.C., 2013. Spatial and temporal variability of the Pacific saury (*Cololabis saira*) distribution in the northwestern Pacific Ocean. *ICES J. Mar. Sci.* 70, 991–999.
- Tseng, C.T., Sun, C.L., Belkin, I.M., Yeh, S.Z., Kuo, C.L., Liu, D.C., 2014. Sea surface temperature fronts affect distribution of Pacific saury (*Cololabis saira*) in the Northwestern Pacific Ocean. *DEEP-SEA Res. PT. II*. 107, 15–21.
- Watanabe, Y., Kurita, Y., Noto, M., Oozeki, Y., Kitagawa, D., 2003. Growth and survival of Pacific saury *Cololabis saira* in the Kuroshio–Oyashio transitional waters. *J. Oceanogr.* 59, 403–414.
- Xu, H., Lennert-Cody, C.E., Maunder, M.N., Minte-Vera, C.V., 2019. Spatiotemporal dynamics of the dolphin-associated purse-seine fishery for yellowfin tuna (*Thunnus albacares*) in the eastern Pacific Ocean. *Fish. Res.* 213, 121–131.
- Yasuda, I., Watanabe, Y., 1994. On the relationship between the Oyashio front and saury fishing grounds in the north-western Pacific: a forecasting method for fishing ground locations. *Fish. Oceanogr.* 3, 172–181.